Interaction-driven transition between topological states in a Kondo insulator

Jan Werner* and Fakher F. Assaad

Institut für Theoretische Physik und Astrophysik, Universität Würzburg, Am Hubland, D-97074 Würzburg, Germany

(Received 26 February 2013; published 11 July 2013)

Heavy fermion materials naturally combine strong spin-orbit interactions and electronic correlations. When there is precisely one conduction electron per impurity spin, the coherent heavy fermion state is insulating. This Kondo insulating state has recently been argued to belong to the class of quantum spin Hall states. Motivated by this conjecture and a very recent experimental realization of this state, we investigate a model for Kondo insulators with spin-orbit coupling. Using dynamical mean-field theory we observe an interaction-driven transition between two distinct topological states, indicated by a closing of the bulk gap and a simultaneous change of topological invariants as obtained in a classification which takes into account lattice symmetries. At large interaction strength we find a topological heavy fermion state, characterized by strongly renormalized heavy bulk bands, hosting a pair of zero-energy edge modes. The model allows a detailed understanding of the temperature dependence of the single particle spectral function and in particular the energy scales at which one observes the appearance of edge states within the bulk gap.

DOI: 10.1103/PhysRevB.88.035113 PACS number(s): 71.27.+a, 71.10.Fd, 03.65.Vf

I. INTRODUCTION

Following the theoretical discovery of the quantum spin Hall (QSH) effect[1–3] and its experimental realization in HgTe quantum well systems[4,5] the field of topological insulators has attracted a lot of research interest. Most intriguing is the fact that this state cannot be connected adiabatically[6] to a conventional insulating state. As a consequence, on the boundary between a topological insulator and a trivial insulator a pair of helical edge modes, which are robust against disorder and interaction effects, emerges.[8,9] The interplay of correlation effects and topology has become a very active field of research.[10] Recently a study of the so-called Kane-Mele-Hubbard model by means of quantum Monte Carlo revealed that the topological insulator phase exists up to rather large values of U before undergoing a continuous phase transition to an antiferromagnetically ordered state, thereby breaking TRS.[11,12] In the disordered phase the interplay of the collective spin mode and topology of the band structure leads to novel effects and model systems.[13,14]

Hubbard-like correlations have equally been included within dynamical mean-field theory (DMFT) for a variety of models including the BHZ model[15] of the QSH effect in HgTe quantum wells.[16–19] At the DMFT level, collective modes are absent and correlation-driven transitions can be understood in terms of a renormalization of the band structure due to a constant real part of the self-energy or due to dynamical effects, which can lead to the divergence of the effective mass.

DMFT is the method of choice to understand the salient temperature dependent features of heavy fermion physics,[20] in particular the coherent heavy fermion state.[21,22] Below the coherence temperature, the individual Kondo screening clouds of the magnetic impurities overlap coherently to form the heavy fermion liquid. This state of matter is adiabatically connected to the non-interacting system and is hence a Fermi liquid. The ultimate signature of coherence in models of heavy fermions is the Kondo insulating state, where there is precisely one conduction electron paired with an impurity spin.[23] Prototypical Kondo insulators are YbB_{12}, CeNiSn, $Ce_3Bi_4Pt_3$, and SmB_6.[24] As proposed in Refs. 25 and 26 a state with a nontrivial band topology may be realized in Kondo insulating systems due to the strong spin-orbit coupling present in these materials, even in the presence of strong electron-electron correlations. In other words, under certain conditions the Kondo insulating state is adiabatically connected to a noninteracting insulator with a nontrivial band topology. This results from the odd-parity wave function of the f electrons,[26] which leads to a nontrivial, momentum-dependent hybridization between f electrons and conduction electrons. Very recently, the Kondo insulator SmB_6 was investigated using an experimental setup suited to identify nonlocal transport effects.[27] A topological Kondo insulating state was indeed found to exist,[27–29] explaining very naturally both the residual conductivity as $T \to 0$ and the existence of in-gap states found in ARPES measurements.[30] Follow-up investigations using a similar method may very well find topologically nontrivial states in other Kondo insulating materials, which are up to now not very well understood.[27]

The aim of this paper is to investigate models of heavy fermions within the DMFT framework which have a topological Kondo insulating ground state. One of our central interests is to assess if this state of matter can occur in the strong coupling local moment regime. In Sec. II we describe our model for topological Kondo insulators. Next we briefly introduce the concept of the topological invariant and explain its evaluation for an interacting system, using the so-called topological Hamiltonian. After describing our method in Sec. IV, we determine the topological properties of the model. In Secs. V and VI we present our main findings, before concluding in Sec. VII.

II. TOPOLOGICAL KONDO INSULATOR

We will devise a model appropriate for Ce-based compounds in two dimensions (2D).[31] Our starting point is the Ce ion's $J = 5/2$ multiplet, which originates from the $4f$ orbitals in the presence of spin-orbit coupling. In the solid state, the multiplet is split further by the crystal electric field, with the splitting depending on the lattice symmetry.[26] We assume that the ground state of the magnetic ion is a Kramer's doublet,

which we call f states. In the simplest case, they hybridize with a single conduction band (d states). With these ingredients we build a model quite similar to the periodic Anderson model (PAM) on a 2D square lattice. The resulting Hamiltonian is

$$\begin{aligned}\mathcal{H} &= \mathcal{H}_0 + \mathcal{H}_U,\\ \mathcal{H}_0 &= \sum_{k\in BZ} \begin{pmatrix} d_k^\dagger \\ f_k^\dagger \end{pmatrix}^T \begin{pmatrix} \boldsymbol{E_d}(k) & V^*\boldsymbol{\Phi}^\dagger(k) \\ V\boldsymbol{\Phi}(k) & \boldsymbol{E}_f(k) \end{pmatrix} \begin{pmatrix} d_k \\ f_k \end{pmatrix}, \qquad (1)\\ \mathcal{H}_U &= U\sum_i n_{i\uparrow}^{(f)} n_{i\downarrow}^{(f)},\end{aligned}$$

where $\boldsymbol{\Phi}(k), \boldsymbol{E}_d(k)$, and $\boldsymbol{E}_f(k)$ are 2×2 submatrices, and encode all the information on the geometry and the effect of spin-orbit coupling. We use $(d_k^\dagger\ f_k^\dagger)$ as a short hand notation for $(d_{k\uparrow}^\dagger\ d_{k\downarrow}^\dagger\ f_{k\uparrow}^\dagger\ f_{k\downarrow}^\dagger)$, creating an electron in the conduction band and the almost localized band, respectively. Here $\uparrow$ and $\downarrow$ denote the pseudospin quantum number.

Due to spin-orbit coupling the f states are eigenstates of the total angular momentum J, and hence hybridize with conduction band states with the same symmetry. This gives rise to the momentum dependence and nontrivial orbital structure of the form-factor $\boldsymbol{\Phi}(k)$.[26] Following the derivation in Ref. 32, we obtain

$$\begin{aligned}\boldsymbol{E}_d(k) &= -2t[\cos(k_x)+\cos(k_y)]\mathbf{1},\\ \boldsymbol{E}_f(k) &= \{\varepsilon_f - 2t_f[\cos(k_x)+\cos(k_y)]\}\mathbf{1},\\ \boldsymbol{\Phi}(k) &= \vec{d}(k)\circ\vec{\boldsymbol{\sigma}},\end{aligned}$$

where

$$\vec{d}(k) = [2\sin(k_x), 2\sin(k_y), 0],$$

formulated in the basis of the Pauli matrices $\vec{\boldsymbol{\sigma}}$ and the 2×2 unit matrix $\mathbf{1}$. The fact that $\boldsymbol{E}_{d,f}(k)$ $[\vec{d}(k)]$ is even (odd) under the transformation $k\to -k$ guarantees time reversal symmetry. The interaction term $\mathcal{H}_U$ acts only on the almost localized f states. The delocalized conduction electrons are only weakly affected by correlation effects, therefore we neglect interactions on the d orbitals. We let the hybridization amplitude take a moderate value of $V = 0.4\,t$, and allow for a small, holelike hopping amplitude between f orbitals, i.e., $t_f = -0.2\,t$. Both will be renormalized to a smaller value in the presence of the interaction.

The noninteracting part of our model can be related to the BHZ model[15,17] for HgTe quantum wells exhibiting the QSH effect. It is given by

$$\begin{aligned}\mathcal{H}(k) &= \begin{pmatrix} \mathcal{H}_{\rm BHZ}(k) & 0 \\ 0 & \mathcal{H}^*_{\rm BHZ}(-k) \end{pmatrix},\\ \mathcal{H}_{\rm BHZ}(k) &= [m-\cos(k_x)-\cos(k_y)]\boldsymbol{\sigma}_z + \lambda[\sin(k_x)\boldsymbol{\sigma}_x\\ &\quad +\sin(k_y)\boldsymbol{\sigma}_y], \qquad (2)\end{aligned}$$

which can be obtained from (1) in the mixed-valence limit $t_f = -t$. The parameters are related by $\lambda = V$ and $m = -\varepsilon_f/4$. Thus we expect some similarities especially in the weak coupling limit. Our primary interest however is the correlation-dominated Kondo insulating state.

III. TOPOLOGICAL INVARIANT

The topological insulator does not connect adiabatically to the trivial band insulator.[8] Both states cannot be characterized by a local order parameter and one has to resort to the concept of a global Z_2 topological invariant $\nu = 0,1$ to distinguish them.[1] Provided that the protecting time reversal symmetry is not broken, states characterized by different values of ν cannot be adiabatically connected without closing the single particle gap. A formulation of the topological invariant in terms of the single-particle Green function[33,34] quite naturally extends the concept to interacting systems adiabatically connected to the noninteracting case.[35] It turns out that the zero-frequency value of the Green function suffices to characterize the state in terms of the topological invariant,[36] which leads to the idea of defining a so-called topological Hamiltonian[37]

$$h_{\rm topo}(k) = -G^{-1}(k, i\omega = 0) = h_0(k) + \Sigma(k, i\omega = 0). \quad (3)$$

The topological invariant of the interacting system is given by the topological invariant corresponding to the noninteracting system governed by the topological Hamiltonian $h_{\rm topo}$. It characterizes correctly the system in terms of the topological invariant, but it does not provide realistic quasiparticle spectra.[37] In the presence of inversion symmetry, the calculation of the topological invariant of (3) is even further simplified.[38] One simply has to calculate the quantity

$$\delta_i = \prod_m \xi_{2m}(\Gamma_i), \qquad (4)$$

where m is the band index and Γ_i are the four time reversal invariant momenta in 2D, namely Γ, M and the equivalent X and Y. ξ_{2m} is the corresponding parity eigenvalue at Γ_i of the $2m$th band. The Z_2 topological invariant is then obtained via

$$(-1)^\nu = \prod_i \delta_i. \qquad (5)$$

As already noted in Ref. 38, the presence of inversion symmetry generates new topological invariants since each of the δ_i acquires a gauge independent meaning. This idea has been pushed further to include the space-group thereby providing an even finer symmetry classification of topological insulators.[39] As the parities are conserved, the corresponding phases are separated by a quantum phase transition where the bulk band gap closes. In particular, the BHZ model on the square lattice exhibits two distinct, topologically nontrivial phases. The Γ phase with the parities $\delta_i = (-1,1,1,1)$ is characterized by a skyrmion structure of the Berry phase centered at zero momentum, while the M phase with $\delta_i = (1,-1,1,1)$ exhibits a Berry phase skyrmion at finite momentum, and was therefore termed a "translationally active" topological insulator in Ref. 40. It has different physical properties since only in this phase dislocations can act as a π flux, binding zero-energy modes. In addition, the model may exhibit an insulating phase associated with the equivalent X and Y points with a trivial band topology, which is in fact realized by introducing a long-range hopping.[39]

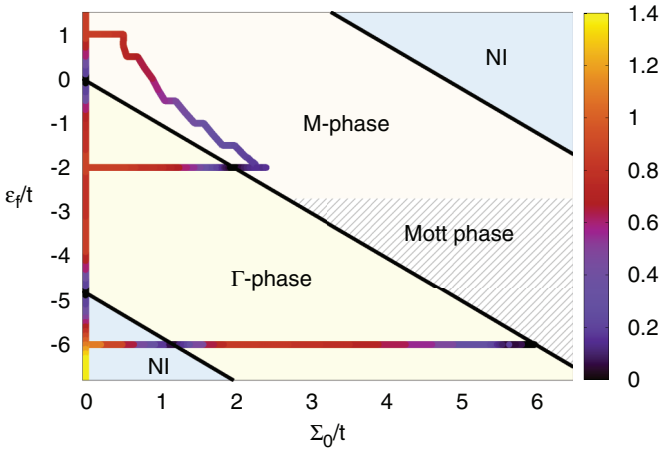

FIG. 1. (Color online) Phase diagram of the topological Hamiltonian (7) for $t_f = -0.2\,t$. On the lines where the right-hand side of Eq. (8) evaluates to zero, the topological invariant is not defined, and the system is in a gapless, semimetallic state. The colored, thick lines represent the simulation runs for different ε_f and U and the analytical results at $U = 0$ were $\Sigma_0 = 0$. The line color corresponds to the band gap size Δ_g. The actual gap closings coincide very well with the predicted transition lines. In a certain part of phase space, instead of the M phase, a possible nontopological Mott phase was found. There the colored lines end. NI denotes the trivial insulator.

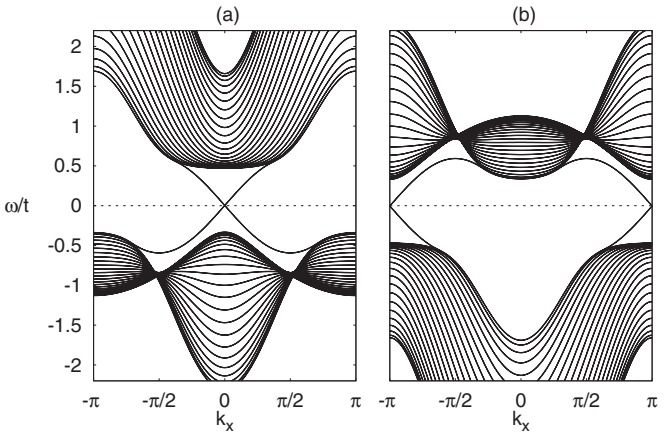

FIG. 2. Band dispersion for the noninteracting case with open boundaries in the y direction: (a) crossing at Γ and (b) crossing at X. The position of the crossing depends on the gauge used.

IV. METHOD

We employ the DMFT to make our model system (1) accessible to numerical methods.[41] The central approximation of the DMFT is the assumption of a momentum-independent self-energy

$$\Sigma(k, i\omega) \sim \Sigma(i\omega). \tag{6}$$

This approach neglects nonlocal correlations. In addition, as we are interested in the properties of the paramagnetic phase, we do not allow for magnetically ordered states, which would break TRS. This translates to a simplification of the topological Hamiltonian (3), which is now the original Hamiltonian renormalized by a constant

$$h_{\text{topo}}(k) = h_0(k) + \Sigma(i\omega = 0) = h_0(k) + \Sigma_0. \tag{7}$$

We can now find an explicit formula for the Z_2 topological invariant (5) in terms of our model's bare parameters and the renormalization constant Σ_0:

$$\begin{aligned}(-1)^{\nu} = {} & \text{sign}(\varepsilon_f + \Sigma_0)^2\, \text{sign}(4t - 4t_f - \Sigma_0 - \varepsilon_f) \\ & \times \text{sign}(4t_f - 4t - \Sigma_0 - \varepsilon_f).\end{aligned} \tag{8}$$

The resulting phase diagram in terms of ε_f and Σ_0 is shown in Fig. 1. It represents a road map, which simplifies the characterization of the system's state once $\Sigma_0 = \Sigma_0(U)$ is known. The simplification (6) allows for a mapping of the lattice problem (1) to an auxiliary single-impurity problem, which describes a fully correlated impurity $\mathcal{H}_{\text{imp}}$ coupled to a noninteracting bath. It can be formulated in terms of an effective action

$$S_{\text{eff}} = \int d\tau d\tau'\, f^{\dagger}(\tau)\mathbf{\Delta}(\tau - \tau') f(\tau') + \int d\tau\, \mathcal{H}_{\text{imp}}(\tau). \tag{9}$$

The bath parameters $\mathbf{\Delta}(\tau)$ have to be obtained in a self-consistent manner. Once convergence is reached, the impurity self-energy is equivalent to the local self-energy $\Sigma(i\omega)$ of the original system.

We use the numerically exact CT-HYB quantum Monte Carlo algorithm[42,43] as the impurity solver at low but finite temperature, which yields the self-energy in imaginary frequency. The inverse temperature was chosen as $\beta t = 100$ in most cases, while close to the transitions it was increased up to $\beta t = 300$.

In the Fermi liquid regime $\text{Im}[\Sigma(i\omega)] \sim i\omega$, while the real part can be extrapolated reliably to a finite value, i.e., $\text{Re}[\Sigma(i\omega \to 0)] = \Sigma_0$. From the local one-particle Green's function in imaginary time $G_{\text{loc}}(\tau) \simeq \exp(\tau\varepsilon_{\pm})$ we infer the position of the upper and lower band edges $\varepsilon_{\pm}$. This method fails when the band gap size becomes comparable to or smaller than the finite simulation temperature.

V. TRANSITION BETWEEN DISTINCT TOPOLOGICAL STATES

In Fig. 1 the phase diagram of the topological Hamiltonian is shown, superimposed with numerical results for the evolution of the band gap size Δ_g as a function of $\Sigma_0(U)$ for different values of ε_f. Positioning the bare f level at $\varepsilon_f = -2.0\,t$ puts the system in a topological insulating state at $U = 0$, with a bulk band gap $\Delta_g \approx 0.88\,t$. On a geometry with open boundaries or with an interface to a conventional insulator, this leads to the formation of a pair of zero-energy edge modes inside the bulk gap, as depicted in Fig. 2.

This state is equivalent to the Γ phase of the BHZ model. As we slowly increase U, the system stays in this phase as long as the bulk gap remains open and TRS is not broken spontaneously. The results for the bulk band gap size Δ_g are shown in Fig. 3. While increasing U, we adapt the position of the chemical potential μ to always stay approximately in the center of the band gap. This way we also ensure that the system is precisely half-filled. Approaching $U = 4.0\,t$, the size of the band gap smoothly decreases, and the gap eventually closes. In this parameter range the band gap is too small to be reliably

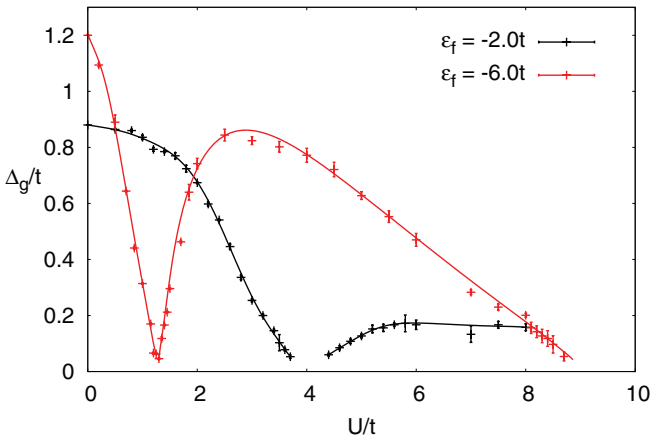

FIG. 3. (Color online) Evolution of the bulk band gap with increasing U for different values of ε_f. The solid curves are guides to the eye.

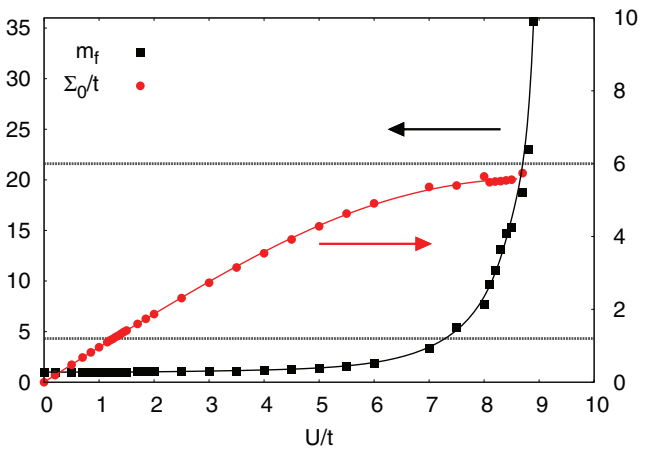

FIG. 4. (Color online) Evolution of the renormalization constant Σ_0 and the effective mass m_f with increasing U for $\varepsilon_f = -6.0\,t$. The horizontal lines indicate the predicted transition lines to the Γ phase at $\Sigma_0 = 1.2\,t$ and the M phase at $\Sigma_0 = 6.0\,t$ obtained from (8). The solid curves are guides to the eye.

calculated with the above method. As a result, the values for the band gap size around $U = 4.0\,t$ were not included in Fig. 3.

Right at $U = 4.0\,t$ the system is in a semimetallic state where the topological invariant is not defined, and can therefore change discontinuously while crossing this point in phase space. In the phase diagram of Fig. 1 this point is exactly on the black, singular line given by $\Sigma_0 = -\varepsilon_f$. Increasing U even further leads to a reopening of the band gap. The calculation of the topological invariant using the topological Hamiltonian (7) reveals that for $U > 4.0\,t$ the system is still in a topological insulating state. Not surprisingly, it is distinct from the state at $U = 0$. Due to the band gap closing at $U = 4.0\,t$, an adiabatic connection to the Γ phase is not possible. Instead this state is connected to a different topological state, namely the one present for $\varepsilon_f > 0$. This state is in fact equivalent to the M phase of the BHZ model. The adiabatic connection can indeed be established by smoothly changing ε_f and U in a way, such that the system stays in this phase. This is done in a simulation run starting at $\varepsilon_f = -2.0\,t$, $U = 6.0\,t$, which corresponds to $\Sigma_0 \approx 2.3\,t$, and evolving the parameters to $\varepsilon_f = +1.0\,t$ and $U = 0$, while staying well away from the singular line $\Sigma_0 = -\varepsilon_f$. Along this path we find no gap closing, as the uppermost colored, somewhat wiggly line in Fig. 1 clearly shows. We explicitly calculated the parities δ_i and found agreement with the combination of parities of the Γ phase and the M phase, respectively. This signifies that at $U = 4.0\,t$ we observe a transition between these two distinct topological states, which is driven by the interaction.

VI. HEAVY BAND TOPOLOGICAL INSULATOR

One can think of other paths in the phase diagram of the topological Hamiltonian. For the choice $\varepsilon_f = -6.0\,t$ the noninteracting system is an insulator with a trivial band topology. The weakly dispersing f band is separated from the d band by a band gap $\Delta_g \approx 1.2\,t$. Smoothly increasing U leads to a phase transition to the Γ phase once the transition line in Fig. 1, defined by $\Sigma_0 = 4t_f - 4t - \varepsilon_f$, is reached, which is the case at $U \approx 1.25\,t$. Indeed, this transition is the one observed in Refs. 17 and 44 in the BHZ-Hubbard model for $m > 2$ at weak coupling strengths. Beyond the semimetallic transition point, as the system is driven deeper into the topological insulator phase, the band gap size increases. It starts to decrease again beyond $U = 3.0\,t$. For values of $U > 8.0\,t$ the bulk band gap size becomes very small, signaling the proximity to the next transition line, which separates the two distinct topological insulator states of Γ phase and M phase. Figure 4 reveals that the renormalization constant $\Sigma_0(U)$ depends on U in a nonlinear way. As we increase U beyond the value of $U = 8.0\,t$, the evolution of Σ_0 becomes very flat. While it approaches the value of $\Sigma_0 = 6.0\,t$, where the transition should happen, the effective mass, as defined by

$$m_f = 1 - \frac{d\,\mathrm{Im}\,\Sigma(\omega)}{d\omega}\Big|_{\omega\to 0} \approx 1 - \frac{\mathrm{Im}\,\Sigma(i\omega_0)}{\omega_0} \qquad (10)$$

increases rapidly, and apparently diverges at $U \approx 8.9\,t$. As a consequence, $\mathrm{Im}[\Sigma(i\omega)]$ remains finite in the limit $\omega \to 0$, indicating a possible orbital-selective Mott transition of the heavy band due to local dynamical fluctuations,[45] or a transition to an antiferromagnetic state, which cannot be captured in our approach. The possibility of a TRS breaking transition is supported by the fact that the f band is exactly half-filled at this point, while the double occupancy is strongly suppressed. The nature of the transition and the phase lying beyond the transition cannot be investigated with our current method. Most probably, due to the approximation of DMFT, in our simulations the size of the band gap becomes so small that it cannot be resolved, but it never closes.[17,46]

To quantify the importance of correlations, and especially to pin down the local moment regime, it is interesting to investigate the quantity

$$\Theta = 1 - \frac{\langle n_\uparrow^{(f)} n_\downarrow^{(f)} \rangle}{\langle n_\uparrow^{(f)} \rangle \langle n_\downarrow^{(f)} \rangle}, \qquad (11)$$

where $\Theta = 0$ without correlations. For a local moment, where the double occupancy is completely suppressed, $\Theta = 1$. Thus we can use this quantity as a measure for the impact of correlations on the system. The evolution of Θ as a function of

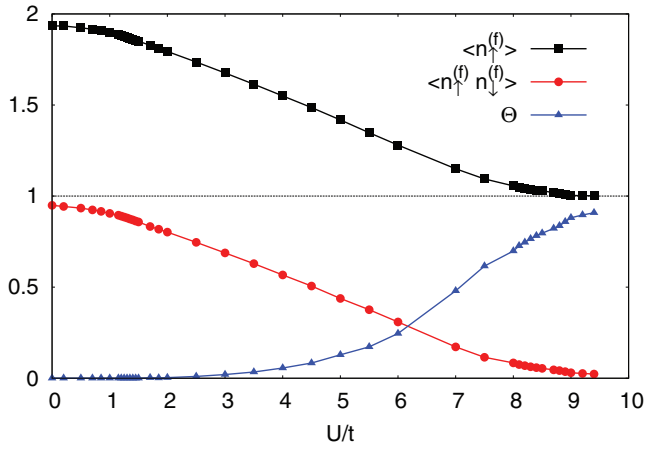

FIG. 5. (Color online) f-level occupancy, double occupancy, and the measure of correlation Θ for $\varepsilon_f = -6.0\,t$ as a function of U.

U is plotted in Fig. 5. With increasing U, the occupancy of the f states decreases. The double occupancy drops even faster, resulting in an increase of Θ. In the range of the transition to the Γ phase at $U \approx 1.25\,t$, the effect of correlations is still negligible, i.e., the transition can also be predicted using a mean-field decoupling of the interaction Hamiltonian $\mathcal{H}_U$.[17] As the f orbitals approach half-filling, correlation effects become very pronounced, as is indicated by the measure of correlation Θ taking values close to 1.

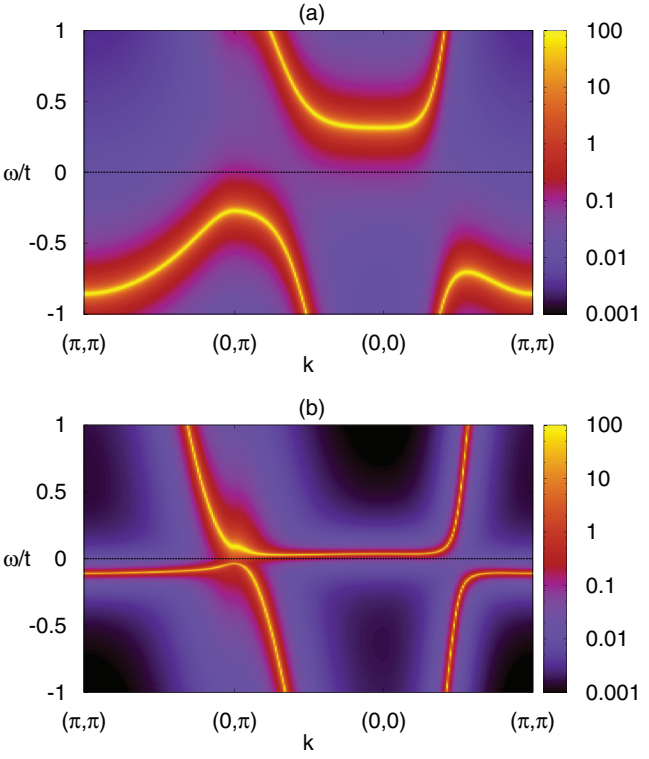

FIG. 6. (Color online) Low energy part of the spectral function for $\varepsilon_f = -6.0\,t$, with an artificial broadening $\delta = 0.01$. The interaction strength is (a) $U = 5.0\,t$, which results in band gap of size $\Delta_g \approx 0.63\,t$ and (b) $U = 8.2\,t$ with $\Delta_g \approx 0.14\,t$. Clearly visible is the formation of the heavy, almost flat bands in the strongly correlated case.

Thus we have a regime of well-defined localized moments on the f orbitals for parameters $U > 8.0\,t$, and a small band gap $\Delta_g \ll t$ separating the weakly dispersing heavy bands. This becomes manifest also in the spectral function $A(k,\omega) = -\pi^{-1}\,\mathrm{Im\,Tr}\,G(k,\omega + i\delta)$. In the small frequency limit we can expand the self-energy $\Sigma(\omega) \approx \Sigma(\omega = 0) + \omega \frac{d\Sigma(\omega)}{d\omega}|_{\omega=0}$. This way we obtain the low-energy spectrum, as shown in Fig. 6(a) for the Γ phase with weak correlations, and in Fig. 6(b) with the strongly renormalized, almost flat bands of the Kondo insulating state, separated by a small gap $\Delta_g \sim T_{\mathrm{coh}}$.

VII. DISCUSSION AND CONCLUSIONS

We have described and studied within the DMFT approximation a model relevant for the understanding of topological Kondo insulators. The concept of the topological Hamiltonian (3) provides a phase diagram which serves as a road map for the interpretation of the numerical results, as long as an adiabatic connection to a noninteracting state exists. The low-temperature phase diagram was found to be very rich. In particular, it is possible to study a transition via an intermediate semimetallic state between two distinct topological states, the Γ phase and the M phase, which is driven by the interaction, and which was not observed previously. With open boundaries, the two states exhibit zero-energy edge modes crossing at $k_x = 0$ and $k_x = \pm\pi$, respectively. The different nature of the two topological states was evidenced by establishing the adiabatic connection to the respective noninteracting states, and by directly calculating the parities corresponding to the time-reversal invariant momenta. Starting from a trivial insulating state at $U = 0$, we can equally observe an interaction-driven transition to the Γ phase. This aspect is similar to investigations of the BHZ-Hubbard model. There the same correlation-driven transition from a trivial to topological insulator was found.[17,44]

All observed zero-temperature phases adiabatically connect to noninteracting states. It is however important to note that the topological state survives well into the local moment regime. This regime is characterized by strongly renormalized bands and a small band gap characteristic of Kondo insulators. The realization of this state of matter in a simple toy model allows the detailed study of the temperature evolution of the single particle spectral function on various topologies with and without edges. In particular, such studies will provide a detailed understanding of the emergence of edge states as the temperature crosses the relevant energy scales of Kondo physics. This will become of increasing importance once a Kondo insulating state is realized in Ce-based surface systems or thin films.[31] Our study is not limited to the two-dimensional case, and can likewise provide insight into three-dimensional topological Kondo insulators. Again of particular interest is the temperature dependence of the single particle spectral function as well as the nature, weak or strong, of the topological state. Studies along these lines are presently under progress.

ACKNOWLEDGMENTS

J.W. would like to thank the Elite Network of Bavaria for funding. F.F.A. thanks the DFG for financial support under the grant proposal AS120/6-1 (FOR1162). We thank the Jülich Supercomputing Centre for allocation of CPU time.

*jwerner@physik.uni-wuerzburg.de

[1] C. L. Kane and E. J. Mele, Phys. Rev. Lett. **95**, 146802 (2005).
[2] C. L. Kane and E. J. Mele, Phys. Rev. Lett. **95**, 226801 (2005).
[3] B. A. Bernevig and S.-C. Zhang, Phys. Rev. Lett. **96**, 106802 (2006).
[4] M. König, S. Wiedmann, C. Brüne, A. Roth, H. Buhmann, L. W. Molenkamp, X.-L. Qi, and S.-C. Zhang, Science **318**, 766 (2007).
[5] A. Roth, C. Brüne, H. Buhmann, L. W. Molenkamp, J. Maciejko, X.-L. Qi, and S.-C. Zhang, Science **325**, 294 (2009).
[6] Adiabatically means that no band gap closing or symmetry breaking occurs.[7]
[7] P. W. Anderson, *Basic Notions Of Condensed Matter Physics* (Benjamin/Cummings, New York, 1984).
[8] X.-L. Qi and S.-C. Zhang, Rev. Mod. Phys. **83**, 1057 (2011).
[9] M. Hohenadler and F. F. Assaad, Phys. Rev. B **85**, 081106 (2012).
[10] M. Hohenadler and F. F. Assaad, J. Phys.: Condens. Matter **25**, 143201 (2013).
[11] M. Hohenadler, T. C. Lang, and F. F. Assaad, Phys. Rev. Lett. **106**, 100403 (2011).
[12] M. Hohenadler, Z.-Y. Meng, T. C. Lang, S. Wessel, A. Muramatsu, and F. F. Assaad, Phys. Rev. B **85**, 115132 (2012).
[13] T. Grover and A. Vishwanath, arXiv:1206.1332.
[14] F. F. Assaad, M. Bercx, and M. Hohenadler, Phys. Rev. X **3**, 011015 (2013).
[15] B. A. Bernevig, T. L. Hughes, and S.-C. Zhang, Science **314**, 1757 (2006).
[16] T. Yoshida, S. Fujimoto, and N. Kawakami, Phys. Rev. B **85**, 125113 (2012).
[17] L. Wang, X. Dai, and X. C. Xie, Europhys. Lett. **98**, 57001 (2012).
[18] T. Yoshida, R. Peters, S. Fujimoto, and N. Kawakami, Phys. Rev. B **87**, 085134 (2013).
[19] J. C. Budich, R. Thomale, G. Li, M. Laubach, and S.-C. Zhang, Phys. Rev. B **86**, 201407 (2012).
[20] T. Pruschke, R. Bulla, and M. Jarrell, Phys. Rev. B **61**, 12799 (2000).
[21] K. S. D. Beach and F. F. Assaad, Phys. Rev. B **77**, 205123 (2008).
[22] L. C. Martin, M. Bercx, and F. F. Assaad, Phys. Rev. B **82**, 245105 (2010).
[23] H. Tsunetsugu, M. Sigrist, and K. Ueda, Rev. Mod. Phys. **69**, 809 (1997).
[24] G. Aeppli and Z. Fisk, Comments Condens. Matter Phys. **16**, 155 (1992).
[25] M. Dzero, K. Sun, V. Galitski, and P. Coleman, Phys. Rev. Lett. **104**, 106408 (2010).
[26] M. Dzero, K. Sun, P. Coleman, and V. Galitski, Phys. Rev. B **85**, 045130 (2012).
[27] S. Wolgast, C. Kurdak, K. Sun, J. W. Allen, D.-J. Kim, and Z. Fisk, arXiv:1211.5104.
[28] X. Zhang, N. P. Butch, P. Syers, S. Ziemak, R. L. Greene, and J. Paglione, Phys. Rev. X **3**, 011011 (2013).
[29] J. Botimer, D. J. Kim, S. Thomas, T. Grant, Z. Fisk, and J. Xia, arXiv:1211.6769.
[30] H. Miyazaki, T. Hajiri, T. Ito, S. Kunii, and S. I. Kimura, Phys. Rev. B **86**, 075105 (2012).
[31] M. Klein, A. Nuber, H. Schwab, C. Albers, N. Tobita, M. Higashiguchi, J. Jiang, S. Fukuda, K. Tanaka, K. Shimada *et al.*, Phys. Rev. Lett. **106**, 186407 (2011).
[32] M.-T. Tran, T. Takimoto, and K.-S. Kim, Phys. Rev. B **85**, 125128 (2012).
[33] Z. Wang, X.-L. Qi, and S.-C. Zhang, Phys. Rev. Lett. **105**, 256803 (2010).
[34] Z. Wang and S.-C. Zhang, Phys. Rev. X **2**, 031008 (2012).
[35] J. C. Budich and B. Trauzettel, Phys. Status Solidi **7**, 109 (2013).
[36] Z. Wang and S.-C. Zhang, Phys. Rev. B **86**, 165116 (2012).
[37] Z. Wang and B. Yan, J. Phys.: Condens. Matter **25**, 155601 (2013).
[38] L. Fu and C. L. Kane, Phys. Rev. B **76**, 045302 (2007).
[39] R.-J. Slager, A. Mesaros, V. Juričić, and J. Zaanen, Nat. Phys. **9**, 98 (2013).
[40] V. Juričić, A. Mesaros, R.-J. Slager, and J. Zaanen, Phys. Rev. Lett. **108**, 106403 (2012).
[41] A. Georges, G. Kotliar, W. Krauth, and M. J. Rozenberg, Rev. Mod. Phys. **68**, 13 (1996).
[42] P. Werner, A. Comanac, L. de Medici, M. Troyer, and A. J. Millis, Phys. Rev. Lett. **97**, 076405 (2006).
[43] P. Werner and A. J. Millis, Phys. Rev. B **74**, 155107 (2006).
[44] J. C. Budich, B. Trauzettel, and G. Sangiovanni, Phys. Rev. B **87**, 235104 (2013).
[45] L. Wang, X. Dai, and X. C. Xie, Phys. Rev. B **84**, 205116 (2011).
[46] K. S. D. Beach and F. F. Assaad, Phys. Rev. B **83**, 045103 (2011).